AIMS Mathematics, 11(6): 18280–18303.
DOI: 10.3934/math.2026743
Received: 25 April 2026
Revised: 08 June 2026
Accepted: 11 June 2026
Published: 22 June 2026

https://www.aimspress.com/journal/Math

Research article

Adaptive and non-adaptive boundary stabilization of the generalized Kuramoto–Sivashinsky equation

N. Smaoui[1,*], **E. Almufadhal**[1], **and R. Al Jamal**[2]

[1] Department of Mathematics, Faculty of Science, Kuwait University, Sabah Al Salem University City, P.O. Box 5969, Safat 13060, Shadadiya, Kuwait

[2] College of Integrative Studies, Abdullah Al Salem University, Khaldiya, Kuwait

* **Correspondence:** Email: n.smaoui@ku.edu.kw.

Abstract: This paper investigates the boundary stabilization of the generalized Kuramoto–Sivashinsky (GKS) equation on a bounded domain. A zero-mean formulation is first introduced to eliminate the spatial drift and to provide a suitable framework for control design. Several nonlinear non-adaptive boundary feedback laws are then proposed and shown, via Lyapunov-based analysis, to guarantee global exponential stability of the closed-loop system in $L^2(0,1)$ when the system parameters are known. To address the case of uncertain coefficients, adaptive boundary feedback laws are subsequently developed, allowing the feedback gains to be adjusted dynamically while preserving exponential stabilization. Numerical simulations are presented to validate the theoretical results and to demonstrate the effectiveness of the proposed controllers. A comparative study between the best-performing adaptive and non-adaptive boundary control laws is also provided, highlighting the trade-off between convergence speed and robustness with respect to parameter uncertainty. Finally, for completeness, a derivation of the GKS equation corresponding to the case $n = 4$ is also presented.

Keywords: generalized Kuramoto–Sivashinsky equation; boundary control; adaptive control; nonlinear partial differential equations
Mathematics Subject Classification: 35K55, 35B35, 93D15, 93C20, 35Q93

1. Introduction

The generalized Kuramoto–Sivashinsky (GKS) equation considered in this work is given by

$$u_t + \alpha u_{xx} + \nu u_{xxxx} + \alpha u^n u_x = 0, \qquad x \in (0, L),\ t > 0, \tag{1.1}$$

where $\alpha, \nu > 0$, $n \geq 1$, and $L > 0$ denotes the length of the spatial interval.

When $n = 1$, Eq (1.1) reduces to the classical Kuramoto–Sivashinsky (KS) equation, which has become a prototypical model describing the interaction between destabilizing long-wave effects and higher-order dissipation. The equation was originally derived by Kuramoto and Tsuzuki [1] in the context of reaction–diffusion systems and flame-front propagation, and independently by Sivashinsky [2] in the study of combustion processes. It later appeared in the modeling of thin liquid film flows [3] and weakly turbulent interfaces [4].

From the perspective of nonlinear dynamics, the KS equation exhibits a rich spectrum of behaviors that depend strongly on the system parameters and the size of the spatial domain. These include stationary solutions, periodic motions, traveling-wave patterns, and chaotic regimes. Analytical studies have established important properties of the system, such as the existence of global attractors and the characterization of its long-time dynamics [5]. Reduced dynamical descriptions on the center-unstable manifold, together with bifurcation analyses, were developed in [6]. In addition, numerical studies have provided insight into the intricate modal interactions that govern the evolution of the system [7,8]. Although the KS equation is an infinite-dimensional partial differential equation (PDE), its asymptotic dynamics are often governed by only a finite number of dominant modes. This property has made it a prototypical model for connecting infinite-dimensional PDE dynamics with low-dimensional nonlinear dynamical systems [9–11].

Building on the observation that the long-time dynamics are often governed by a finite number of dominant modes, reduced-order modeling and data-driven approaches have also been employed to analyze KS-type dynamics and identify the dominant modes governing their evolution [12–14]. More recently, machine-learning and physics-informed computational methods have emerged as powerful tools for the numerical approximation of complex PDEs. Examples include adaptive neural-network-based approaches for time-fractional diffusion equations and related nonlinear systems, which combine data-driven learning with the underlying physical structure of the governing equations [15]. Although the present work focuses on analytical stabilization and control rather than learning-based numerical techniques, these developments highlight the growing diversity of methodologies available for the study of nonlinear PDEs.

Beyond the classical KS equation, a natural extension is provided by the GKS equation, which incorporates more general nonlinear mechanisms and may exhibit even richer dynamical behavior. Spectral and numerical investigations of GKS-type models were carried out in [16–18]. Exact solutions and traveling-wave structures were studied in [19–21], while the influence of stochastic perturbations and various dynamical properties of KS-type equations were investigated in [22, 23]. Further studies addressed nonlinear stability of periodic waves and other dynamical features of the system [24, 25].

Because KS equations exhibit intrinsic instabilities and can evolve toward chaotic regimes, the problem of stabilizing their dynamics has attracted considerable attention. Various feedback control strategies have been proposed, including distributed control approaches [26–28], boundary stabilization methods [29–31], and reduced-order control designs [32, 33]. Adaptive control mechanisms capable of adjusting to uncertain parameters have also been investigated in [34, 35].

For the GKS equation, several works have addressed stabilization of steady states and feedback regulation using optimal- or actuator-based control strategies [36, 37]. More recently, feedback control designs for the nonlinear GKS equation have been explored in [38–40]. Despite these advances, many existing approaches rely on linearized models, reduced-order approximations, or finite-dimensional representations of the dynamics. Consequently, rigorous stabilization results for

the full nonlinear infinite-dimensional GKS equation remain relatively limited. Furthermore, the design of boundary feedback controllers capable of handling uncertain or unknown system parameters has received comparatively little attention. These limitations motivate the development of stabilization strategies that operate directly on the nonlinear infinite-dimensional system while accommodating parameter uncertainty.

Motivated by these challenges, this paper investigates the boundary stabilization of the GKS equation using both non-adaptive and adaptive feedback control strategies. The non-adaptive framework assumes that the physical parameters of the system are known, whereas the adaptive framework is designed to cope with uncertainty in the viscosity coefficient ν and the convective coefficient α.

The main contributions of this work are threefold. First, a zero-mean reformulation of the GKS equation is introduced, providing a convenient framework for the Lyapunov-based stability analysis. Second, nonlinear boundary feedback laws are developed for the full nonlinear infinite-dimensional GKS equation under both known and unknown system parameters. Using Lyapunov-based techniques and suitable energy estimates, global exponential stabilization of the resulting closed-loop systems is established. In the adaptive case, augmented Lyapunov functionals are constructed to establish boundedness of the adaptive gains and exponential stabilization of the closed-loop system despite parameter uncertainty. Third, representative numerical simulations are presented to assess the effectiveness of the proposed controllers and to compare the performance of the adaptive and non-adaptive strategies. In addition, a derivation of the GKS equation corresponding to the case $n = 4$ is provided in Appendix A, extending previously available derivations for the cases $n = 1, 2$, and $n = 3$ (see, e.g., [41, 42]).

The results presented here contribute to the understanding of boundary stabilization for higher-order nonlinear dissipative PDEs and highlight the role of adaptive feedback mechanisms in controlling complex spatio-temporal dynamics governed by KS-type systems.

The remainder of the paper is organized as follows. Section 2 presents the problem formulation and introduces the zero-mean representation of the GKS equation, which removes the drift component and provides a convenient framework for the subsequent stability analysis. Section 3 investigates the non-adaptive boundary control problem. In this section, four nonlinear non-adaptive boundary controllers are proposed, and their stabilization properties are analyzed. Representative numerical simulations are also presented to illustrate the effectiveness of the proposed controllers and to compare their convergence behavior. Section 4 is devoted to the adaptive boundary control design. Three adaptive boundary controllers are developed to address the case where the system parameters are unknown. Stability analysis together with representative numerical simulations are provided to demonstrate the effectiveness of the adaptive strategies and to compare their behavior. In Section 5, a comparative study between the adaptive and non-adaptive boundary control approaches is carried out in order to highlight their respective performance and convergence properties. Finally, Section 6 summarizes the main findings of the paper and presents concluding remarks. For completeness, the derivation of the GKS equation for the case $n = 4$ is provided in Appendix A.

2. Model reformulation

We consider the GKS equation introduced in the Introduction,

$$u_t + \alpha u_{xx} + \nu u_{xxxx} + \alpha u^n u_x = 0, \qquad x \in (0, L),\ t > 0, \tag{2.1}$$

where $\alpha, \nu > 0$, $n \geq 1$, and $L > 0$.

Introducing the potential variable $v(x, t)$ such that $u = v_x$ in (2.1) and integrating with respect to x, we obtain the potential form

$$v_t + \nu v_{xxxx} + \alpha \left(v_{xx} + \frac{1}{n+1} (v_x)^{n+1} \right) = C(t), \tag{2.2}$$

where $C(t)$ is a function of integration.

Let

$$m(t) = \frac{1}{L} \int_0^L v(x, t)\, dx$$

denote the spatial mean of v.

To facilitate the stability analysis, we introduce a zero-mean reformulation of the GKS equation. This transformation removes the drift component associated with the spatial average of the solution and facilitates the use of standard functional inequalities in the subsequent Lyapunov analysis.

Introducing the zero-mean variable

$$w(x, t) = v(x, t) - m(t),$$

and substituting into (2.2), we obtain

$$w_t + \nu w_{xxxx} + \alpha \left(w_{xx} + \frac{1}{n+1} (w_x)^{n+1} \right) + \frac{dm}{dt} = C(t). \tag{2.3}$$

Defining the modified mean function

$$\widetilde{m}(t) = m(t) - \int_0^t C(s)\, ds,$$

it follows that

$$\frac{d\widetilde{m}}{dt} = \frac{dm}{dt} - C(t).$$

Therefore, the zero-mean form of the GKS equation becomes

$$w_t + \nu w_{xxxx} + \alpha \left(w_{xx} + \frac{1}{n+1} (w_x)^{n+1} \right) + \frac{d\widetilde{m}}{dt} = 0. \tag{2.4}$$

Equation (2.4) serves as the starting point for the boundary control design developed in the subsequent sections.

Remark 2.1. *Since $w(x,t)$ satisfies the zero-mean condition*

$$\int_0^L w(x,t)\,dx = 0,$$

the Poincaré inequality for zero-mean functions on bounded intervals (see, e.g., [11]) yields:

$$\|w(\cdot,t)\|_{L^2(0,L)} \le \frac{L}{\pi}\|w_x(\cdot,t)\|_{L^2(0,L)}. \tag{2.5}$$

Therefore, exponential decay of $\|w_x(\cdot,t)\|_{L^2(0,L)}$ implies exponential decay of $\|w(\cdot,t)\|_{L^2(0,L)}$.

Remark 2.2. *The well-posedness of the GKS equation on bounded domains has been extensively studied in the literature. Under suitable boundary conditions and sufficiently regular initial data, the system admits a unique global solution; see, for example, [28, 39] and the references therein. Throughout this work, solutions are assumed to belong to the standard Sobolev spaces associated with the GKS equation, ensuring that the required boundary values and integrations by parts used in the Lyapunov analysis are well defined. It should be emphasized that these regularity assumptions are standard in the analysis of nonlinear PDEs and are imposed solely to justify the mathematical arguments employed in the stability proofs. They do not exclude the possibility of complex or chaotic dynamics in the uncontrolled system, since such dynamics may still occur within the corresponding Sobolev spaces.*

For the uncontrolled system, we consider Eq (2.4) on $(0,1)\times(0,T)$ subject to

$$w_x(0,t) = w_{xx}(0,t) = 0, \tag{2.6}$$

$$w_{xxx}(1,t) = w_{xxxx}(1,t) = 0, \tag{2.7}$$

with initial condition

$$w(x,0) = w_0(x). \tag{2.8}$$

3. Non-adaptive boundary feedback laws

In this section, we construct four nonlinear boundary feedback laws that exponentially stabilize the zero-mean GKS equation

$$w_t + \nu w_{xxxx} + \alpha\left(w_{xx} + \frac{1}{n+1}(w_x)^{n+1}\right) + \frac{d\widetilde{m}}{dt} = 0, \qquad x\in(0,1),\ t>0, \tag{3.1}$$

subject to

$$w_x(0,t) = 0, \qquad w_{xx}(0,t) = 0, \tag{3.2}$$

$$w_{xxx}(1,t) = g(t), \qquad w_{xxxx}(1,t) = h(t), \tag{3.3}$$

where $\nu,\alpha>0$ and $n\ge 1$.

We define the Lyapunov functional $V: H^1(0,1)\to\mathbb{R}$ by

$$V(t) = \frac{1}{2}\int_0^1 w_x^2(x,t)\,dx. \tag{3.4}$$

The following lemma provides a general Lyapunov estimate that will be used repeatedly in the analysis of the proposed non-adaptive boundary feedback laws.

Lemma 3.1. *Let w be a sufficiently smooth solution of* (3.1)–(3.3) *so that the boundary values and integrations by parts used below are well defined. If $\eta = \nu - \alpha > 0$, then the Lyapunov functional* (3.4) *satisfies*

$$\dot{V} \leq -\nu w_x w_{xxxx}|_0^1 + \nu w_{xx} w_{xxx}|_0^1 - \alpha w_x w_{xx}|_0^1 - \frac{\alpha}{n+2} w_x^{n+2}\Big|_0^1 - 2\eta V. \tag{3.5}$$

Proof. Differentiating (3.4) with respect to t gives

$$\dot{V}(t) = \int_0^1 w_x w_{xt}\, dx.$$

Since $\dfrac{d\tilde{m}}{dt}$ is independent of x, differentiating (3.1) with respect to x yields

$$w_{xt} = -\nu w_{xxxxx} - \alpha w_{xxx} - \alpha (w_x)^n w_{xx}.$$

Therefore,

$$\dot{V} = -\nu \int_0^1 w_x w_{xxxxx}\, dx - \alpha \int_0^1 w_x w_{xxx}\, dx - \alpha \int_0^1 w_x^{n+1} w_{xx}\, dx. \tag{3.6}$$

We now compute each term in (3.6). For the fourth-order dissipative term, applying integration by parts twice yields

$$-\nu \int_0^1 w_x w_{xxxxx}\, dx = -\nu w_x w_{xxxx}|_0^1 + \nu w_{xx} w_{xxx}|_0^1 - \nu \int_0^1 w_{xxx}^2\, dx.$$

Similarly,

$$-\alpha \int_0^1 w_x w_{xxx}\, dx = -\alpha w_x w_{xx}|_0^1 + \alpha \int_0^1 w_{xx}^2\, dx,$$

while

$$-\alpha \int_0^1 w_x^{n+1} w_{xx}\, dx = -\frac{\alpha}{n+2} w_x^{n+2}\Big|_0^1.$$

Combining the preceding identities, we obtain

$$\dot{V} = -\nu \int_0^1 w_{xxx}^2\, dx + \alpha \int_0^1 w_{xx}^2\, dx - \nu w_x w_{xxxx}|_0^1 + \nu w_{xx} w_{xxx}|_0^1 - \alpha w_x w_{xx}|_0^1 - \frac{\alpha}{n+2} w_x^{n+2}\Big|_0^1. \tag{3.7}$$

Using the boundary conditions $w_x(0,t) = 0$ and $w_{xx}(0,t) = 0$, together with the Poincaré-type inequalities

$$\int_0^1 w_x^2\, dx \leq \int_0^1 w_{xx}^2\, dx \leq \int_0^1 w_{xxx}^2\, dx,$$

we get

$$-\nu \int_0^1 w_{xxx}^2\, dx + \alpha \int_0^1 w_{xx}^2\, dx \leq -(\nu - \alpha) \int_0^1 w_x^2\, dx.$$

Since $\eta = \nu - \alpha > 0$ and

$$V(t) = \frac{1}{2}\int_0^1 w_x^2\,dx,$$

we have

$$-(\nu-\alpha)\int_0^1 w_x^2\,dx = -2\eta V(t).$$

Substituting this estimate into (3.7), we obtain

$$\dot{V} \le -\nu w_x w_{xxx}|_0^1 + \nu w_{xx}w_{xx}|_0^1 - \alpha w_x w_{xx}|_0^1 - \frac{\alpha}{n+2}w_x^{n+2}\Big|_0^1 - 2\eta V,$$

which proves (3.5). □

3.1. First feedback law

Consider (3.1) and (3.2) with

$$\begin{cases} w_{xxx}(1,t) = g(t) = -K_1 w_{xx}^k(1,t), \\ w_{xxxx}(1,t) = h(t) = -\frac{1}{\nu}\left[\alpha w_{xx}(1,t) + \frac{\alpha}{n+2}w_x^{n+1}(1,t) - K_2 w_x^k(1,t)\right], \end{cases} \tag{3.8}$$

where $K_1, K_2 > 0$ and k is an odd positive integer.

Theorem 3.1. *Let $\nu > \alpha > 0$. Then the closed-loop system defined by* (3.1)*,* (3.2)*, and* (3.8) *is globally exponentially stable in $L^2(0,1)$.*

Proof. Using the boundary conditions $w_x(0,t) = 0$ and $w_{xx}(0,t) = 0$ given in (3.2), and substituting the boundary control laws (3.8) into (3.5), we obtain

$$\begin{aligned}\dot{V} \le{}& \alpha w_x(1,t)w_{xx}(1,t) + \frac{\alpha}{n+2}w_x^{n+2}(1,t) - K_2 w_x^{k+1}(1,t) \\ &- \nu K_1 w_{xx}^{k+1}(1,t) - \alpha w_x(1,t)w_{xx}(1,t) - \frac{\alpha}{n+2}w_x^{n+2}(1,t) - 2\eta V.\end{aligned}$$

The terms involving $w_x(1,t)w_{xx}(1,t)$ and $w_x^{n+2}(1,t)$ cancel, and therefore

$$\dot{V} \le -K_2 w_x^{k+1}(1,t) - \nu K_1 w_{xx}^{k+1}(1,t) - 2\eta V.$$

Since k is odd, $k+1$ is even, implying

$$w_x^{k+1}(1,t) \ge 0, \qquad w_{xx}^{k+1}(1,t) \ge 0.$$

Hence

$$\dot{V} \le -2\eta V.$$

By Grönwall's inequality,

$$V(t) \le V(0)e^{-2\eta t}.$$

Since

$$V(t) = \frac{1}{2}\int_0^1 w_x^2(x,t)\,dx,$$

it follows that $\|w_x(\cdot,t)\|_{L^2(0,1)}$ decays exponentially. The conclusion then follows from the Poincaré inequality (2.5), which implies exponential decay in $L^2(0,1)$. □

3.2. Second feedback law

Consider (3.1) and (3.2) with

$$\begin{cases} w_{xxx}(1,t) = g(t) = \frac{1}{\nu}\left[\alpha w_x(1,t) - K_1 w_{xx}^k(1,t)\right], \\ w_{xxxx}(1,t) = h(t) = -\frac{1}{\nu}\left[\frac{\alpha}{n+2} w_x^{n+1}(1,t) - K_2 w_x^k(1,t)\right], \end{cases} \tag{3.9}$$

where $K_1, K_2 > 0$ and k is an odd positive integer.

Theorem 3.2. *Let $\nu > \alpha > 0$. Then the closed-loop system defined by* (3.1)*,* (3.2)*, and* (3.9) *is globally exponentially stable in $L^2(0,1)$.*

Proof. Using the Lyapunov functional (3.4) and substituting the boundary control law (3.9) into (3.5), we obtain

$$\dot{V} \leq -K_2 w_x^{k+1}(1,t) - K_1 w_{xx}^{k+1}(1,t) - 2\eta V \leq -2\eta V.$$

The conclusion follows as in the previous theorem. □

3.3. Third feedback law

Consider (3.1)–(3.2) with

$$\begin{cases} w_{xxx}(1,t) = g(t) = -\frac{1}{\nu} K_2 w_x(1,t), \\ w_{xxxx}(1,t) = h(t) = -\frac{1}{\nu}\left[\frac{\alpha}{n+2} w_x^{n+1}(1,t) + K_4 w_{xx}(1,t)\right], \end{cases} \tag{3.10}$$

where $K_2, K_4 > 0$.

Theorem 3.3. *Let $\nu > \alpha > 0$ and choose $K_4 = K_2 + \alpha$. Then the closed-loop system defined by* (3.1)*,* (3.2)*, and* (3.10) *is globally exponentially stable in $L^2(0,1)$.*

Proof. Proceeding as before with the Lyapunov functional (3.4), substitution of the boundary control law (3.10) into (3.5) yields

$$\dot{V} \leq (K_4 - K_2 - \alpha) w_x(1,t) w_{xx}(1,t) - 2\eta V.$$

Choosing $K_4 = K_2 + \alpha$ yields

$$\dot{V} \leq -2\eta V.$$

The rest follows as before. □

3.4. Fourth feedback law

Consider (3.1) and (3.2) with

$$\begin{cases} w_{xxx}(1,t) = g(t) = 0, \\ w_{xxxx}(1,t) = h(t) = \frac{1}{\nu}\left[K_3 w_x^k(1,t) - \alpha w_{xx}(1,t) - \frac{\alpha}{n+2} w_x^{n+1}(1,t)\right], \end{cases} \tag{3.11}$$

where $K_3 > 0$ and k is an odd positive integer.

Theorem 3.4. *Let $\nu > \alpha > 0$. Then the closed-loop system defined by* (3.1)*,* (3.2)*, and* (3.11) *is globally exponentially stable in $L^2(0,1)$.*

Proof. Applying the Lyapunov functional (3.4) and substituting the boundary control law (3.11) into (3.5), we get $\dot{V} \leq -K_3 w_x^{k+1}(1,t) - 2\eta V \leq -2\eta V$, since $k+1$ is even. Hence, the result follows from Grönwall's inequality and (2.5). □

3.5. Numerical simulations and comparison of the non-adaptive boundary controllers

The numerical simulations presented in this paper were carried out using COMSOL Multiphysics 6.3 through the General Form PDE interface. Spatial discretization was performed using the finite element method (FEM) with quadratic Lagrange shape functions. The computational domain $(0, 1)$ was discretized using a uniform one-dimensional mesh consisting of 50 finite elements and 51 mesh vertices. Owing to the fourth-order nature of the GKS equation, an extra-fine mesh was used to accurately resolve the solution dynamics. Time integration was performed using the backward differentiation formula (BDF) solver available in COMSOL. The BDF method is an implicit multi-step scheme for solving initial-value problems and is particularly well suited for stiff differential equations. In the simulations, a maximum BDF order of five was employed together with a time step of $\Delta t = 0.001$. The simulations were carried out over the prescribed time interval, and the numerical solutions were found to be stable and insensitive to further mesh refinement and reductions in the time step.

We illustrate the behavior of the uncontrolled and controlled GKS equation through numerical simulations. The initial condition $w_0(x) = \sin(\pi x)$ is chosen to illustrate the qualitative stabilization behavior of the proposed controllers. Although this initial condition does not exactly satisfy the boundary condition $w_x(0, t) = 0$ at $t = 0$, the numerical solution rapidly adjusts to the imposed boundary conditions, and the resulting long-term controlled dynamics remain unaffected. The simulations are performed using the parameter values $\alpha = 0.0001$, $\nu = 0.001$, and nonlinear orders $n = 1, 2$.

We first consider the uncontrolled problem obtained by setting the right-end boundary inputs equal to zero. Figure 1 shows that, for both $n = 1$ and $n = 2$, the solution norm $\|w_x(\cdot, t)\|$ grows rapidly, indicating instability of the open-loop dynamics.

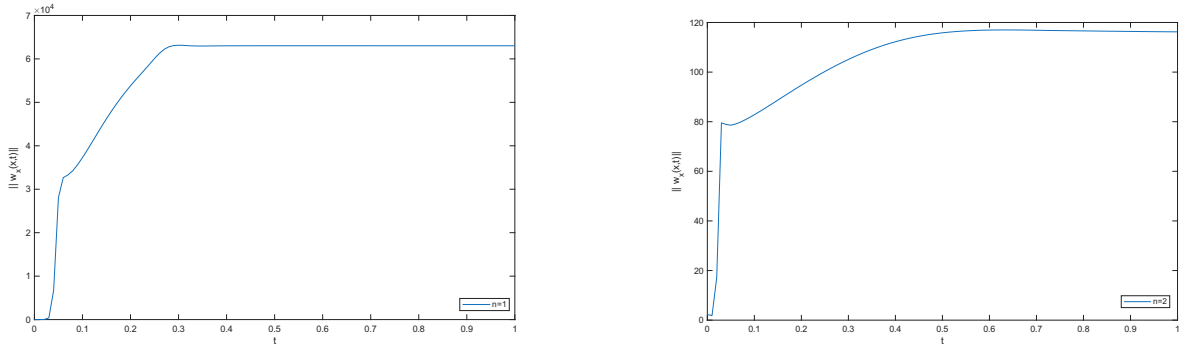

(a) **(b)**

Figure 1. The L^2-norm of $w_x(x, t)$ versus time for the uncontrolled system with $n = 1$ and $n = 2$, for $\nu = 0.001$, $\alpha = 0.0001$, and $w_0(x) = \sin(\pi x)$: (a) $n = 1$, (b) $n = 2$.

All four feedback laws stabilize the system, in agreement with the theoretical results established in Theorems 3.1–3.4. To avoid unnecessary repetition, we present only one representative controlled evolution in the main text. Figure 2 illustrates the decay of the solution and its spatial derivative under the third feedback law, which yields the fastest convergence among the four controllers considered.

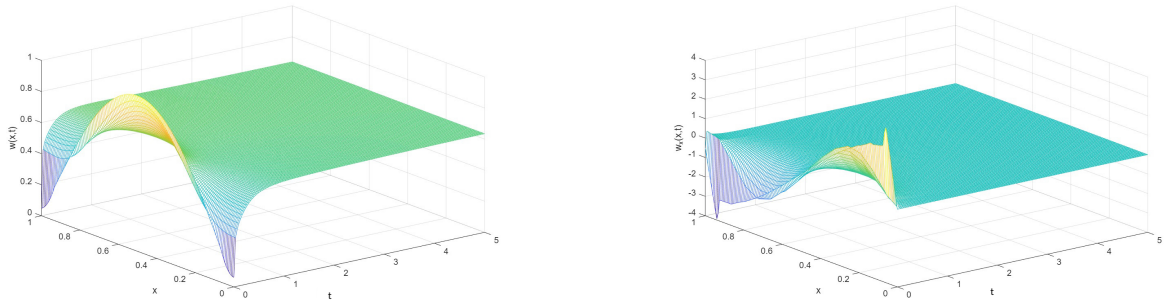

(a) **(b)**

Figure 2. Representative three-dimensional evolution of (a) $w(x,t)$ and (b) $w_x(x,t)$ under the third nonlinear non-adaptive two-input control law in Theorem 3.3, with parameters $\nu = 0.001$, $\alpha = 0.0001$, $k = 1$, $K_2 = 1$, $n = 1$, and $w_0(x) = \sin(\pi x)$.

To facilitate a direct comparison among the four feedback laws, we plot $\|w_x(\cdot,t)\|$ for the same parameter values as in the uncontrolled case, with the controller gains fixed at $K_1 = K_2 = K_3 = 1$.

Figure 3 and Figure 4 present the time evolution of $\|w_x(\cdot,t)\|$ and its logarithm for the third control law, which yields the fastest decay for $n = 1$ and $n = 2$. Table 1 reports the convergence times for the four controllers. The results show that the third control law yields the fastest decay, followed by the second and first laws, whereas the one-input fourth law produces the slowest convergence.

Table 1. Approximate convergence times of the four non-adaptive boundary controllers.

Control law	$n = 1$	$n = 2$
Theorem 3.1	10.5 s	10.5 s
Theorem 3.2	5.0 s	5.0 s
Theorem 3.3	3.7 s	3.7 s
Theorem 3.4	11.6 s	11.6 s

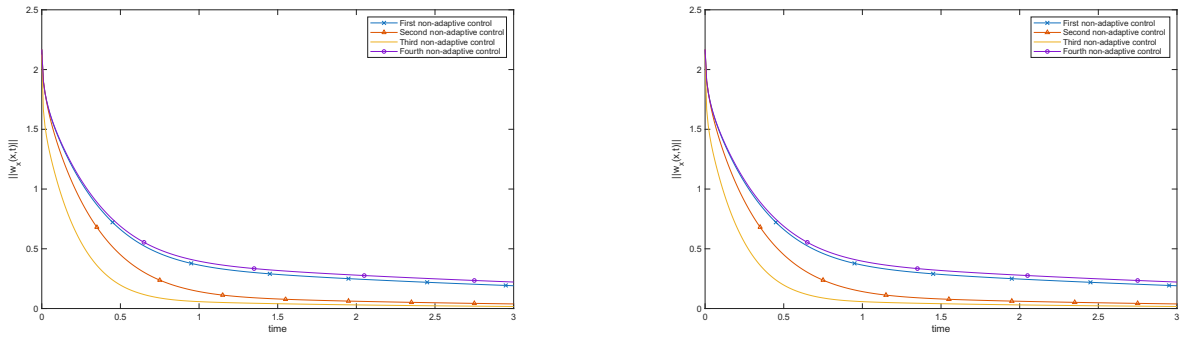

(a) **(b)**

Figure 3. Comparison of the L^2-norm of $w_x(x,t)$ versus time for $n = 1$ and $n = 2$ under the four non-adaptive boundary feedback laws, with parameters $\nu = 0.001$, $\alpha = 0.0001$, $k = 1$, $w_0(x) = \sin(\pi x)$, and $K_1 = K_2 = K_3 = 1$: (a) $n = 1$, (b) $n = 2$.

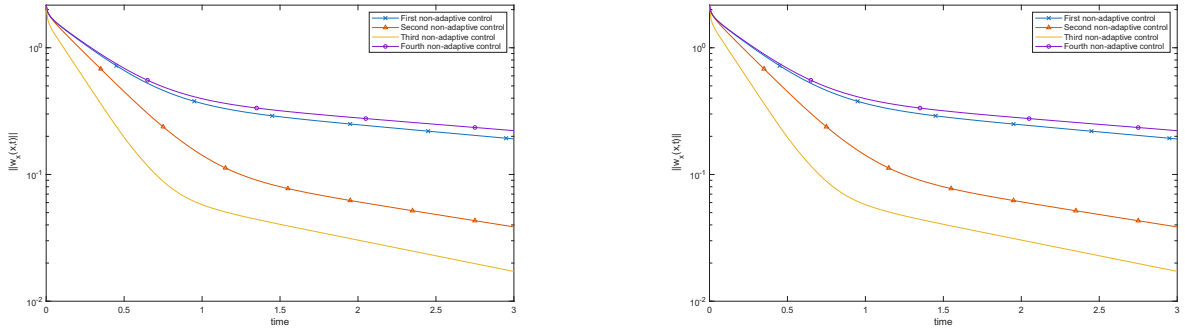

(a) **(b)**

Figure 4. Comparison of the L^2-norm of the natural logarithm of $w_x(x,t)$ versus time for $n = 1$ and $n = 2$ under the four non-adaptive boundary feedback laws, with parameters $\nu = 0.001$, $\alpha = 0.0001$, $k = 1$, $w_0(x) = \sin(\pi x)$, and $K_1 = K_2 = K_3 = 1$: (a) $n = 1$, (b) $n = 2$.

4. Adaptive boundary feedback laws

In this section, we design adaptive boundary feedback laws for the zero-mean GKS equation when the coefficients ν and α are unknown positive constants. As in the previous section, we assume that

$$\eta = \nu - \alpha > 0.$$

We consider

$$w_t + \nu w_{xxxx} + \alpha\left(w_{xx} + \frac{1}{n+1}(w_x)^{n+1}\right) + \frac{d\widetilde{m}}{dt} = 0, \qquad x \in (0,1),\ t > 0, \tag{4.1}$$

subject to

$$w_x(0,t) = 0, \qquad w_{xx}(0,t) = 0. \tag{4.2}$$

$$w_{xxx}(1,t) = \tilde{g}(t), \qquad w_{xxxx}(1,t) = \tilde{h}(t). \tag{4.3}$$

We again use the Lyapunov functional $V : H^1(0,1) \to \mathbb{R}$ by

$$V(t) = \frac{1}{2}\int_0^1 w_x^2(x,t)\,dx.$$

By the same calculations as in the non-adaptive section, we have

$$\dot{V} \le -\nu w_x w_{xxx}\big|_0^1 + \nu w_{xx} w_{xx}\big|_0^1 - \alpha w_x w_{xx}\big|_0^1 - \frac{\alpha}{n+2} w_x^{n+2}\Big|_0^1 - 2\eta V. \tag{4.4}$$

Moreover, since the zero-mean formulation is used, and the Poincaré inequality holds for all $t \ge 0$. Hence, exponential decay of $\|w_x(\cdot,t)\|$ implies exponential decay of $\|w(\cdot,t)\|$.

4.1. First adaptive boundary feedback law

Consider (4.1)–(4.3) with

$$\begin{cases} w_{xxx}(1,t) = \tilde{g}(t) = -\eta_1(t)\, w_{xx}(1,t) - w_{xx}(1,t), \\ w_{xxxx}(1,t) = \tilde{h}(t) = \eta_2(t)\, w_x(1,t) + \dfrac{1}{4}\, w_x(1,t) + \eta_3(t)\, w_x^{n+1}(1,t), \end{cases} \tag{4.5}$$

where

$$\dot{\eta}_1 = r_1 w_{xx}^2(1,t), \qquad \dot{\eta}_2 = r_2 w_x^2(1,t), \qquad \dot{\eta}_3 = r_3 w_x^{n+2}(1,t), \qquad r_1, r_2, r_3 > 0. \tag{4.6}$$

Theorem 4.1. *Let $\nu > \alpha > 0$. Then the closed-loop system defined by* (4.1)–(4.3)*,* (4.5)*, and* (4.6) *is globally exponentially stable in $L^2(0,1)$.*

Proof. Consider the Lyapunov functional defined in (3.4). By differentiating V with respect to t and substituting the boundary control law (4.5) into (4.4), we obtain

$$\begin{aligned}\dot{V} \leq & -\nu\eta_2 w_x^2(1,t) - \frac{1}{4}\nu w_x^2(1,t) - \nu\eta_3 w_x^{n+2}(1,t) - \nu\eta_1 w_{xx}^2(1,t) \\ & - \nu w_{xx}^2(1,t) - \alpha w_x(1,t) w_{xx}(1,t) - \frac{\alpha}{n+2} w_x^{n+2}(1,t) - 2\eta V.\end{aligned} \tag{4.7}$$

Using

$$-\nu w_{xx}^2 - \alpha w_x w_{xx} - \frac{1}{4}\nu w_x^2 = -\nu\left(w_{xx} + \frac{\alpha}{2\nu} w_x\right)^2 - \frac{1}{4}\left(\nu - \frac{\alpha^2}{\nu}\right) w_x^2 \leq 0,$$

we deduce that

$$\dot{V} \leq -2\eta V - \nu\eta_1 w_{xx}^2(1,t) - \nu\eta_2 w_x^2(1,t) - \nu\eta_3 w_x^{n+2}(1,t) - \frac{\alpha}{n+2} w_x^{n+2}(1,t). \tag{4.8}$$

Define the augmented energy function

$$E(t) = V(t) + \frac{\nu}{2r_1}(\eta_1 - a)^2 + \frac{\nu}{2r_2}(\eta_2 - b)^2 + \frac{1}{2r_3\nu}\left(\nu\eta_3 + \frac{\alpha}{n+2}\right)^2, \tag{4.9}$$

where $a, b > 0$. Differentiating (4.9) and using (4.6), we get

$$\dot{E} = \dot{V} + \nu(\eta_1 - a) w_{xx}^2(1,t) + \nu(\eta_2 - b) w_x^2(1,t) + \left(\nu\eta_3 + \frac{\alpha}{n+2}\right) w_x^{n+2}(1,t).$$

Combining this identity with (4.8), we obtain

$$\dot{E} \leq -2\eta V - \nu a\, w_{xx}^2(1,t) - \nu b\, w_x^2(1,t) \leq -2\eta V.$$

Hence, $E(t) \leq E(0)$ for all $t \geq 0$. Since all additional terms in (4.9) are nonnegative, it follows that

$$\frac{\nu}{2r_1}(\eta_1 - a)^2, \qquad \frac{\nu}{2r_2}(\eta_2 - b)^2, \qquad \frac{1}{2r_3\nu}\left(\nu\eta_3 + \frac{\alpha}{n+2}\right)^2$$

remain bounded for all $t \geq 0$. Hence, η_1, η_2, and η_3 are bounded.

The remainder of the proof follows as in [43]. In particular, using the boundedness of the adaptive parameters together with Grönwall's inequality and Lemmas 1 and 2 of [43], it follows that $V(t)$ decays exponentially to zero. The Poincaré inequality then implies that the zero solution is globally exponentially stable in $L^2(0,1)$. □

Remark 4.1. *For all adaptive boundary feedback laws proposed in this section, the adaptive update laws guarantee boundedness of the parameter estimates and exponential stabilization of the closed-loop system. However, the estimated parameters are not necessarily guaranteed to converge to their true values. In general, convergence of the parameter estimates requires additional excitation conditions, such as persistent excitation, which are not assumed in the present work. Therefore, the primary objective of the adaptive laws is to compensate for parameter uncertainty and ensure stabilization of the closed-loop system rather than to identify the exact parameter values.*

4.2. Second adaptive boundary feedback law

Consider (4.1)–(4.3) with

$$\begin{cases} w_{xxx}(1,t) = \tilde{g}(t) = -w_{xx}(1,t), \\ w_{xxxx}(1,t) = \tilde{h}(t) = \eta_2(t)\, w_x(1,t) + \dfrac{1}{4}\, w_x(1,t) + \eta_3(t)\, w_x^{n+1}(1,t), \end{cases} \tag{4.10}$$

where

$$\dot{\eta}_2 = r_2 w_x^2(1,t), \qquad \dot{\eta}_3 = r_3 w_x^{n+2}(1,t), \qquad r_2, r_3 > 0. \tag{4.11}$$

Theorem 4.2. *Let $\nu > \alpha > 0$. Then the closed-loop system defined by* (4.1)–(4.3)*,* (4.10)*, and* (4.11) *is globally exponentially stable in $L^2(0,1)$.*

Proof. Using the Lyapunov functional (3.4), we differentiate V with respect to t and substitute the boundary control law (4.10) into (4.4). Following the same steps as in the proof of Theorem 4.1, we obtain

$$\dot{V} \le -2\eta V - \nu\eta_2 w_x^2(1,t) - \nu\eta_3 w_x^{n+2}(1,t) - \frac{\alpha}{n+2} w_x^{n+2}(1,t). \tag{4.12}$$

Now define

$$E(t) = V(t) + \frac{\nu}{2r_2}(\eta_2 - b)^2 + \frac{1}{2r_3\nu}\left(\nu\eta_3 + \frac{\alpha}{n+2}\right)^2, \tag{4.13}$$

with $b > 0$. Differentiating (4.13) and using (4.11), we obtain

$$\dot{E} = \dot{V} + \nu(\eta_2 - b) w_x^2(1,t) + \left(\nu\eta_3 + \frac{\alpha}{n+2}\right) w_x^{n+2}(1,t).$$

Therefore,

$$\dot{E} \le -2\eta V - \nu b\, w_x^2(1,t) \le -2\eta V.$$

Hence, $E(t) \le E(0)$ for all $t \ge 0$. Since all additional terms in (4.13) are nonnegative, it follows that

$$\frac{\nu}{2r_2}(\eta_2 - b)^2, \qquad \frac{1}{2r_3\nu}\left(\nu\eta_3 + \frac{\alpha}{n+2}\right)^2$$

remain bounded for all $t \ge 0$. Hence η_2 and η_3 are bounded. The conclusion follows as in the proof of Theorem 4.1. □

4.3. Third adaptive boundary feedback law

Consider (4.1)–(4.3) with

$$\begin{cases} w_{xxx}(1,t) = \tilde{g}(t) = -w_{xx}(1,t), \\ w_{xxxx}(1,t) = \tilde{h}(t) = \dfrac{1}{4}\, w_x(1,t) + \eta_3(t)\, w_x^{n+1}(1,t), \end{cases} \tag{4.14}$$

where

$$\dot{\eta}_3 = r_3 w_x^{n+2}(1,t), \qquad r_3 > 0. \tag{4.15}$$

Theorem 4.3. *Let $\nu > \alpha > 0$. Then the closed-loop system defined by* (4.1)–(4.3)*,* (4.14)*, and* (4.15) *is globally exponentially stable in $L^2(0,1)$.*

Proof. Using the Lyapunov functional (3.4), we differentiate V with respect to t and substitute the boundary control law (4.14) into (4.4). Arguing as in Theorem 4.1, we get

$$\dot{V} \leq -2\eta V - \nu\eta_3 w_x^{n+2}(1,t) - \frac{\alpha}{n+2} w_x^{n+2}(1,t). \tag{4.16}$$

Define

$$E(t) = V(t) + \frac{1}{2r_3\nu}\left(\nu\eta_3 + \frac{\alpha}{n+2}\right)^2. \tag{4.17}$$

Differentiating (4.17) and using (4.15) yields

$$\dot{E} = \dot{V} + \left(\nu\eta_3 + \frac{\alpha}{n+2}\right) w_x^{n+2}(1,t) \leq -2\eta V.$$

Thus

$$E(t) \leq E(0), \qquad t \geq 0.$$

Since the additional term in (4.17) is nonnegative, it follows that

$$\frac{1}{2r_3\nu}\left(\nu\eta_3 + \frac{\alpha}{n+2}\right)^2$$

remains bounded for all $t \geq 0$. Hence, η_3 remains bounded. The conclusion follows as in the proof of Theorem 4.1. □

4.4. Numerical simulations of the adaptive controllers

The same numerical implementation described in Section 3.5 was used for the adaptive simulations. We now present numerical simulations for the adaptive boundary feedback laws. The simulations were carried out on the domain $t \in [0,5]$ and $x \in [0,1]$, with initial condition $w_0(x) = \sin(\pi x)$. Unless otherwise stated, the parameter values were chosen as $\nu = 0.001$, $\alpha = 0.0001$, and $r_1 = r_2 = r_3 = 50$.

All three adaptive controllers stabilize the system without requiring prior knowledge of ν and α. Figure 5 illustrates the controlled evolution under the first adaptive feedback law, which provides the fastest convergence among the three adaptive controllers.

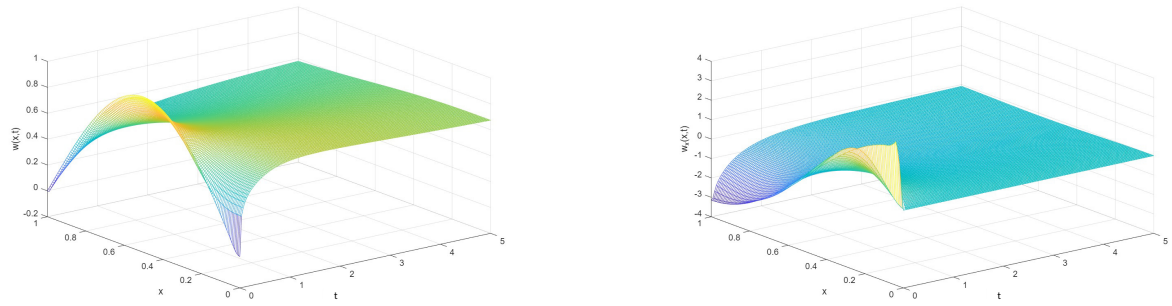

(a) **(b)**

Figure 5. Three-dimensional evolution of (a) $w(x,t)$ and (b) $w_x(x,t)$ under the first nonlinear adaptive control law in Theorem 4.1, with parameters $n = 1$, $\nu = 0.001$, $\alpha = 0.0001$, $r_1 = r_2 = r_3 = 50$, and $w_0(x) = \sin(\pi x)$.

Figures 6 and 7, together with Table 2, compare the three adaptive control laws.

Table 2. Approximate convergence times for the three adaptive boundary control laws.

Adaptive control law	$n = 1$	$n = 2$
Theorem 4.1	9.5 s	10.7 s
Theorem 4.2	12.7 s	13.7 s
Theorem 4.3	14.5 s	16.6 s

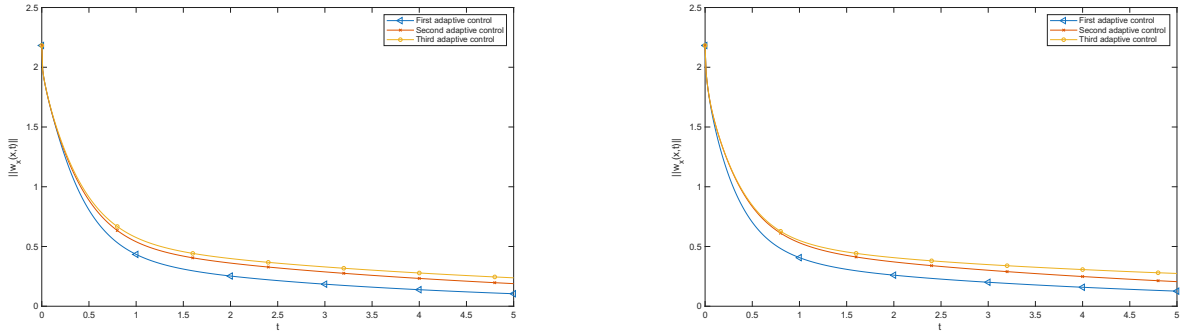

(a) **(b)**

Figure 6. Comparison of the three adaptive control laws in Theorems 4.1–4.3 through the L^2-norm of $w_x(x,t)$ versus time for $n = 1$ and $n = 2$.

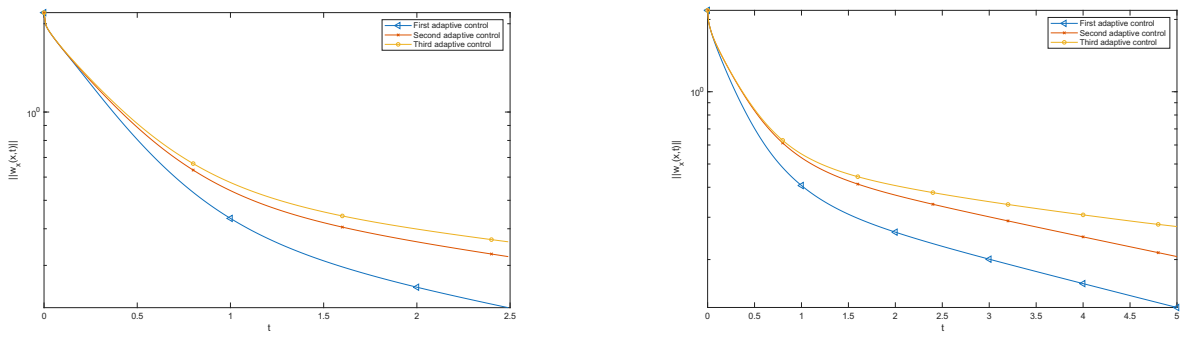

(a) **(b)**

Figure 7. Logarithmic plots of $\|w_x(\cdot,t)\|$ for the three adaptive control laws.

The numerical results confirm that adaptive boundary control provides robust stabilization even in the absence of exact parameter knowledge. However, the convergence rate is slightly slower than that of the best non-adaptive controller.

5. Comparison between adaptive and non-adaptive boundary control strategies

In this section, we compare the performance of the best-performing non-adaptive controller from Section 3 (the third non-adaptive boundary control law) and the best-performing adaptive controller from Section 4 (the first adaptive boundary control law). The comparison focuses on stabilization

speed, robustness to parameter uncertainty, and overall control performance. All simulations are conducted under identical conditions on the domain $t \in [0, 5]$ and $x \in [0, 1]$, with initial condition $w_0(x) = \sin(\pi x)$.

The non-adaptive control laws assume that the parameters ν and α are known *a priori*, allowing the control gains to be fixed in advance. In contrast, the adaptive controllers do not require prior knowledge of these parameters and instead adjust the gains dynamically through adaptation laws. This feature makes the adaptive strategy particularly attractive in situations where the system parameters are uncertain or difficult to measure.

The numerical simulations show that both adaptive and non-adaptive control strategies successfully stabilize the solution of the GKS equation, in agreement with the theoretical results established in Sections 3 and 4. In all cases, the L^2-norm $\|w_x(\cdot, t)\|$ decays to zero, while the logarithmic plots exhibit an approximately linear profile, confirming exponential convergence of the controlled solution.

Among the adaptive controllers, the first adaptive boundary control law provides the fastest convergence, followed closely by the second adaptive law, whereas the third adaptive law exhibits a slightly slower decay rate. This behavior may be partly attributed to the number of adaptive parameters involved in each design, since the first controller updates three gains simultaneously, allowing greater flexibility in compensating for the system dynamics.

A direct comparison between the adaptive and non-adaptive controllers is presented in Figures 8 and 9, which show the time evolution of $\|w_x(\cdot, t)\|$ and its logarithm for the representative cases $n = 1$ and $n = 2$. In both cases, the controlled solution decays monotonically, confirming stabilization of the system. However, the best-performing non-adaptive controller achieves faster convergence than the best-performing adaptive controller, as reflected by the steeper decay observed in the plots.

For both $n = 1$ and $n = 2$, the non-adaptive controller produces a noticeably faster decay of $\|w_x(\cdot, t)\|$ over the considered time interval, whereas the adaptive controller exhibits a more gradual convergence. This indicates that the improved transient performance of the non-adaptive controller is not restricted to a particular choice of the nonlinearity exponent.

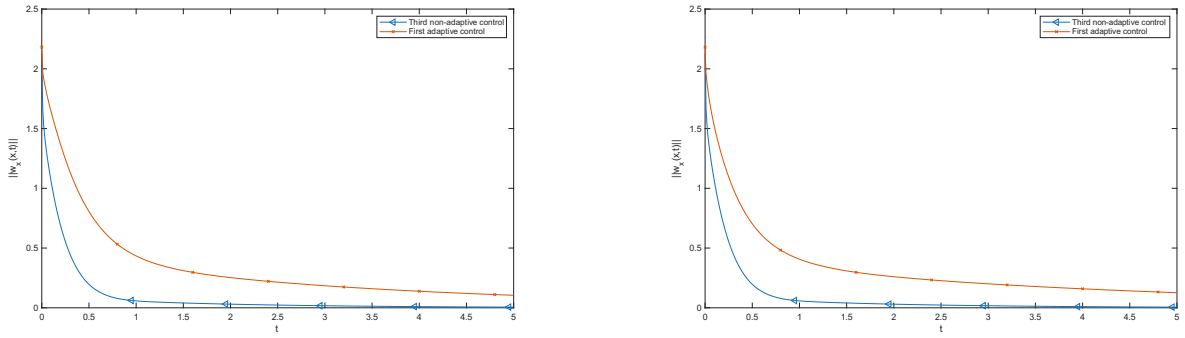

(a) **(b)**

Figure 8. Comparison between the best-performing adaptive and non-adaptive boundary controllers obtained in Sections 4 and 3, respectively. The figure shows the time evolution of the L^2-norm $\|w_x(\cdot, t)\|$ for the GKS equation, illustrating the stabilization performance of the two controllers. The parameters are $\alpha = 0.0001$, $\nu = 0.001$, $r_1 = r_2 = r_3 = 50$, $K_2 = 1$, and $w_0(x) = \sin(\pi x)$. (a) $n = 1$; (b) $n = 2$.

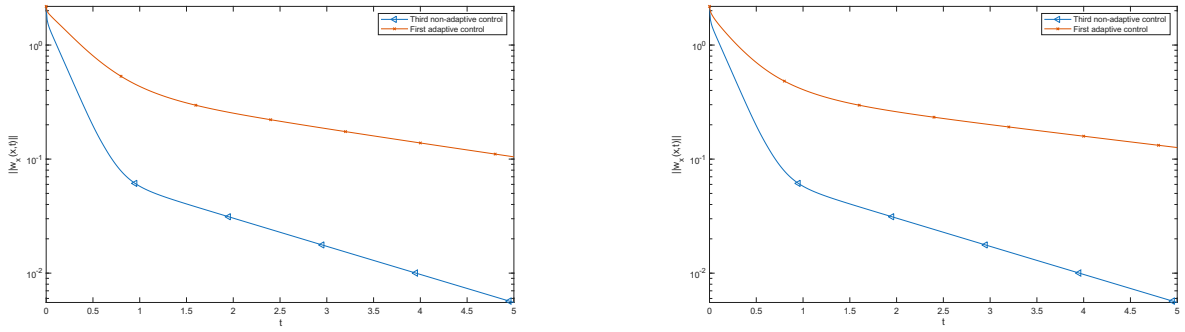

(a) **(b)**

Figure 9. Comparison between the best-performing adaptive and non-adaptive boundary controllers obtained in Sections 4 and 3, respectively. The figure displays the time evolution of $\ln \|w_x(\cdot, t)\|$ for the GKS equation, highlighting the approximately linear decay that confirms exponential stabilization. The parameters are $\alpha = 0.0001$, $\nu = 0.001$, $r_1 = r_2 = r_3 = 50$, and $K_2 = 1$, and the initial condition is $w_0(x) = \sin(\pi x)$. (a) $n = 1$; (b) $n = 2$.

These results highlight an important trade-off between the two control strategies. When the system parameters are known, the non-adaptive controller achieves faster stabilization because its gains are designed directly from the model coefficients. On the other hand, the adaptive controller offers a significant practical advantage by guaranteeing stabilization without requiring prior knowledge of the system parameters. Therefore, while the non-adaptive controller provides better transient performance for known systems, the adaptive controller offers greater robustness and flexibility in the presence of parameter uncertainty.

Remark 5.1. *The proposed boundary control laws exhibit complementary advantages in terms of applicability and robustness. The non-adaptive controller is suitable when the system parameters are known or can be accurately estimated, and it typically yields faster stabilization rates, as demonstrated by the numerical results. In contrast, the adaptive controller is designed to accommodate parameter uncertainty through online adjustment of the controller gains, thereby eliminating the need for precise prior knowledge of the system parameters. Consequently, the adaptive strategy provides enhanced robustness with respect to uncertain parameters while still guaranteeing exponential stabilization of the closed-loop system. Since the control design relies primarily on Lyapunov-based energy estimates and boundary actuation, the methodology may also be extended to other nonlinear dissipative PDEs with similar structural properties.*

Remark 5.2. *The proposed control laws belong to the class of Lyapunov-based boundary feedback controllers for nonlinear PDEs. Compared with optimization-based approaches, such as model predictive control, the present methodology provides explicit feedback laws together with rigorous exponential stability guarantees. Similarly, compared with backstepping-based designs, the proposed controllers avoid the construction and solution of kernel equations while still ensuring exponential stabilization of the closed-loop system. In contrast to data-driven and machine-learning-based control strategies, the design is derived directly from the mathematical structure of the governing equation and does not require training data. Furthermore, unlike reduced-order-model-based controllers, the proposed approach is developed directly for the infinite-dimensional system, thereby avoiding issues associated with model reduction accuracy and spillover effects. The adaptive*

boundary controller additionally accommodates parameter uncertainty through online parameter adjustment while preserving the stability properties of the closed-loop system.

6. Conclusions

In this paper, boundary feedback control strategies were developed for the stabilization of the GKS equation on a bounded domain. Several non-adaptive boundary feedback laws were first constructed and shown, through Lyapunov analysis, to ensure global exponential stability when the system parameters are known. Adaptive boundary feedback laws were then proposed to address the case of unknown parameters while preserving the exponential stability of the closed-loop system.

Numerical simulations were performed to demonstrate the effectiveness of both classes of controllers. The results showed that all proposed feedback laws successfully stabilize the system and drive the solution toward the zero equilibrium. Among the non-adaptive controllers, the third control law exhibited the fastest convergence, whereas among the adaptive controllers, the first adaptive law provided the best overall performance. A direct comparison between the best non-adaptive and adaptive controllers highlighted the expected trade-off between convergence speed and robustness: non-adaptive strategy achieves faster convergence when the system parameters are known *a priori*, whereas the adaptive strategy guarantees stabilization without requiring prior knowledge of the physical parameters.

Future research will focus on several extensions of the present work, including the design of boundary control laws for broader classes of nonlinear dissipative PDEs, the incorporation of external disturbances and measurement uncertainties, and the quantitative assessment of the control effort associated with the adaptive and non-adaptive controllers through suitable control-energy metrics.

Finally, for completeness, a derivation of the GKS equation corresponding to the case $n = 4$ was included, thereby extending the modeling framework associated with the class of equations considered in this work.

Author contributions

Nejib Smaoui: Conceptualization, Methodology, Visualization, Formal analysis, Data curation, Software, Writing-original draft; Writing-review and editing, Supervision; Eilaf Almufadhal: Formal analysis, Data Curation, Software, Writing-review and editing; Rasha Al Jamal: Formal analysis, Writing-review and editing. All authors have read and approved the final version of the manuscript for publication.

Use of Generative-AI tools declaration

The authors declare that they have not used Artificial Intelligence (AI) tools in the creation of this article.

Conflict of interest

The authors declare that they have no competing interests.

References

1. Y. Kuramoto, T. Tsuzuki, Persistent propagation of concentration waves in dissipative media far from thermal equilibrium, *Prog. Theor. Phys.*, **55** (1976), 356–369. https://doi.org/10.1143/PTP.55.356
2. G. I. Sivashinsky, On flame propagation under conditions of stoichiometry, *SIAM J. Appl. Math.*, **39** (1980), 67–82. https://doi.org/10.1137/0139007
3. L. Chen, H. Chang, Nonlinear waves on liquid film surfaces–II. Bifurcation analyses of the ling-wave equation, *Chem. Eng. Sci.*, **41** (1986), 2477–2486. https://doi.org/10.1016/0009-2509(86)80033-1
4. J. M. Hyman, B. Nicolaenko, S. Zaleski, Order and complexity in the Kuramoto-Sivashinsky model of weakly turbulent interface, *Phys. D*, **23** (1986), 265–292. https://doi.org/10.1016/0167-2789(86)90136-3
5. B. Nicolaenko, B. Scheurer, R. Temam, Some global dynamical properties of the Kuramoto-Sivashinsky equations: Nonlinear stability and attractors, *Phys. D*, **16** (1985), 155–183. https://doi.org/10.1016/0167-2789(85)90056-9
6. D. Armbruster, J. Guckenheimer, P. Holmes, Kuramoto-Sivashinsky dynamics on the center-unstable manifold, *SIAM J. Appl. Math.*, **49** (1989), 676–691. https://doi.org/10.1137/0149039
7. I. G. Kevrekidis, B. Nicolaenko, C. Scovel, Back in the saddle again: A computer assisted study of the Kuramoto-Sivashinsky equation, *SIAM J. Appl. Math.*, **50** (1990), 760–790. https://doi.org/10.1137/0150045
8. M. Kirby, D. Armbruster, Reconstructing phase space for PDE simulations, *Z. Angew. Math. Phys.*, **43** (1992), 999–1022. https://doi.org/10.1007/BF00916425
9. J. Hyman, B. Nicolaenko, The Kuramoto-Sivashinsky equation: A bridge between PDEs and dynamical systems, *Phys. D: Nonlinear Phenom.*, **18** (1986), 113–126. https://doi.org/10.1016/0167-2789(86)90166-1
10. J. Robinson, *Infinite-Dimensional Dynamical Systems*, Cambridge: Cambridge University Press, 2001.
11. R. Temam, *Infinite-Dimensional Dynamical Systems in Mechanics and Physics*, 2 Eds, Berlin: Springer, 1988.
12. N. Smaoui, S. Al-Yakoob, Analyzing the dynamics of cellular flames using Karhunen-Loéve decomposition and autoassociative neural networks, *SIAM J. Sci. Comput.*, **24** (2003), 1790–1808. https://doi.org/10.1137/S1064827501386201
13. N. Smaoui, Artificial neural network-based low-dimensional Model for spatio-temporally varying cellular flames, *Appl. Math. Model.*, **21** (1997), 739–748. https://doi.org/10.1016/S0307-904X(97)00092-9
14. N. Smaoui, Linear versus nonlinear dimensionality reduction of high-dimensional dynamical systems, *SIAM J. Sci. Comput.*, **25** (2004), 2107–2125. https://doi.org/10.1137/S1064827502412723

15. B. Shiri, H. Kong, G. C. Wu, C. Luo, Adaptive learning neural network method for solving time–fractional diffusion equations, *Neur. Comput.*, **34** (2022), 971–990. https://doi.org/10.1162/neco_a_01482

16. B. Guo, X. M. Xiang, The large time convergence of spectral method for generalized Kuramoto-Sivashinsky equations, *J. Comput. Math.*, **15** (1997), 1–13.

17. B. Guo, X. Wu, The spectral method for the generalized Kuramoto-Sivashinsky equation, *J. Comput. Math.*, **9** (1991), 330–336.

18. G. Akrivis, D. T. Papageorgiou, Y. S. Smyrlis, Computational Study of the dispersively modified Kuramoto–Sivashinsky equation, *SIAM J. Sci. Comput.*, **34** (2021), A792–A813. https://doi.org/10.1137/100816791

19. Z. J. Yang, Travelling wave solutions to nonlinear evolution and wave equations, *J. Phys. A: Math. Gen.*, **27** (1994), 2837. https://doi.org/10.1088/0305-4470/27/8/021

20. C. Li, G. Chen, S. Zhao, Exact traveling wave solutions to the generalized Kuramoto-Sivashinsky equation, *Lat. Am. Appl. Res.*, **34** (2004), 64–68.

21. N. A. Kudryashov, Traveling wave solutions of the Kuramoto-Sivashinsky equation with nonlinear convection, *Phys. Lett. A*, **585** (2026), 131644. https://doi.org/10.1016/j.physleta.2026.131644

22. S. Albosaily, W. W. Mohammed, A. Rezaiguia, M. El-Morshedy, E. M. Elsayed, The influence of the noise on the exact solutions of a Kuramoto-Sivashinsky equation, *Open Math.*, **20** (2022), 108–116. https://doi.org/10.1515/math-2022-0012

23. M. Benlahsen, G. Bogna, Z. Csáti, M. Guedda, K. Hriczó, Dynamical properties of a nonlinear Kuramoto–Sivashinsky growth equation, *Alex. Eng. J.*, **60** (2021), 3419–3427. https://doi.org/10.1016/j.aej.2021.02.003

24. N. A. Kudryashov, S. F. Lavrova, Dynamical features of the generalized Kuramoto-Sivashinsky equation, *Chaos Solit. Fract.*, **142** (2021), 110502. https://doi.org/10.1016/j.chaos.2020.110502

25. B. Barker, M. A. Johnson, P. Noble, L. M. Rodrigues, K. Zumbrun, Nonlinear modulational stability of periodic traveling-wave solutions of the generalized Kuramoto–Sivashinsky equation, *Phys. D: Nonlinear Phenom.*, **258** (2013), 11–46. https://doi.org/10.1016/j.physd.2013.04.011

26. P. D. Christofides, A. Armaou, Global stabilization of the Kuramoto-Sivashinsky equation via distributed output feedback control, *Syst. Control Lett.*, **39** (2000), 283–294. https://doi.org/10.1016/S0167-6911(99)00108-5

27. N. Smaoui, A. El-Kadri, M. Zribi, Nonlinear boundary control of the unforced generalized Korteweg-de Vries-Burgers equation, *Nonlinear Dyn.*, **60** (2010), 561–574.

28. R. Al Jamal, K. Morris, Linearized stability of partial differential equations with application to stabilization of the Kuramoto-Sivashinsky equation, *SIAM J. Control Optim.*, **56** (2018), 120–147. https://doi.org/10.1137/140993417

29. R. Sakthivel, H. Ito, Nonlinear robust boundary control of the Kuramoto-Sivashinsky equation, *IMA J. Math. Control Inform.*, **24** (2007), 47–55. https://doi.org/10.1093/imamci/dnl009

30. W. J. Liu, M. Krstic, Stability enhancement by boundary control in the Kuramoto-Sivashinsky equation, *Nonlinear Anal. Theory Meth. Appl.*, **43** (2001), 485–507. https://doi.org/10.1016/S0362-546X(99)00215-1

31. S. Dubljevic, Boundary model predictive control of Kuramoto-Sivashinsky equation with input and state constraints input and state constraints, *Comput. Chem. Eng.*, **34** (2010), 1655–1661.

32. C. Lee, H. Tran, Reduced-order-based feedback control of the Kuramoto-Sivashinsky equation, *J. Comput. Appl. Math.*, **173** (2005), 1–19. https://doi.org/10.1016/j.cam.2004.02.021

33. K. Morris, Design of finite-dimensional controllers for infinite-dimensional systems by approximation, *J. Math. Syst. Estim. Control*, **6** (1994), 151–180.

34. T. Kobayashi, Adaptive stabilization of a class of reaction-diffusion systems, *J. Dyn. Control*, **11** (2001), 47–56. https://doi.org/10.1023/A:1017999917259

35. T. Kobayashi, Adaptive stabilization of the Kuramoto-Sivashinsky equation, *Int. J. Syst. Sci.*, **33** (2002), 175–180. https://doi.org/10.1080/00207720110092171

36. R. Cimpeanu, S. N. Gomes, D. T. Papageorgiou, Active control of liquid films flows: Beyond reduced-order models, *Nonlinear Dyn.*, **104** (2021), 267–287. https://doi.org/10.1007/s11071-021-06287-5

37. S. N. Gomes, D. T. Papageorgiou, G. A. Pavliotis, Stabilizing non-trivial solutions of the generalized Kuramoto–Sivashinsky equation using feedback and optimal control, *IMA J. Appl. Math.*, **82** (2016), 158–194. https://doi.org/10.1093/imamat/hxw011

38. R. Al Jamal, N. Smaoui, A single input-feedback control of the generalized Kuramoto-Sivashinsky equation, In: *3rd IFSA Winter Conference Proceeding ARCI*, 2023, 127–131.

39. R. Al Jamal, N. Smaoui, A single actuator vs. multi-actuator design of an input-feedback control for the generalized Kuramoto–Sivashinsky equation, *Nonlinear Dyn.*, **111** (2023), 19371–19385. https://doi.org/10.1007-023-08861-5

40. R. Al Jamal, N. Smaoui, A single bounded input-feedback control to the generalized Kortweg-de Vries-Burgers-Kuramoto-Sivashinsky equation, *Math. Meth. Appl. Sci.*, **46** (2022), 2222–2248. https://doi.org/10.1002/mma.8640

41. H. Demiray, On the derivation of some non-linear evolution equations and their progressive wave solutions, *Int. J. Non-Linear Mech.*, **38** (2003), 63–70. https://doi.org/10.1016/S0020-7462(01)00042-7

42. N. Smaoui, B. Chentouf, A. Alalabi, Modelling and nonlinear boundary stabilization of the modified generalized Korteweg–de Vries–Burgers equation, *Adv. Differ. Equ.*, **2019** (2019), 449. https://doi.org/10.1186/s13662-019-2376-x

43. N. Smaoui, A. El-Kadri, M. Zribi, Adaptive boundary control of the unforced generalized Korteweg-de Vries-Burgers equation, *Nonlinear Dyn.*, **69** (2012), 1237–1253.

A. Derivation of the generalized Kuramoto–Sivashinsky equation for the case $n = 4$

In this appendix, we derive a GKS equation with fourth-order nonlinearity. The cases corresponding to lower-order nonlinearities, namely $n = 1, 2$, were previously derived by Demiray [41], while the case $n = 3$ was obtained by Smaoui et al. [42]. Here, we extend the same asymptotic framework to derive the case $n = 4$.

We begin with the non-dimensionalized equations governing the propagation of weakly nonlinear waves in a prestressed, thick-walled viscoelastic tube filled with an inviscid fluid:

$$2u_t + (1+u)w_x + 2wu_x = 0, \tag{A.1}$$

$$w_t + ww_x + p_x - \nu\left(\frac{-8w}{(1+u)^2} + w_{xx}\right) = 0, \tag{A.2}$$

supplemented by the non-dimensionalized dynamical pressure relation

$$p = \beta_1 u + \beta_2 u_{xx} + \beta_3 u_{tt} + \beta_4 u_t + \beta_5 u_{xxt} + \beta_6 u^2 + \beta_7 u^3 + \beta_8 u^4 + \cdots . \tag{A.3}$$

The inclusion of the term $\beta_8 u^4$ extends the previously known model and allows the derivation of a fourth-order nonlinear evolution equation.

To carry out the asymptotic reduction, we introduce the stretched variables

$$\mu = \epsilon^{\delta}(x - gt), \qquad \eta = \epsilon^{\delta+\gamma} gt, \tag{A.4}$$

where $\epsilon > 0$ is a small parameter, g denotes the linear wave speed, and $\delta, \gamma > 0$ are scaling parameters. Under this transformation, the dependent variables are expanded as

$$u = \sum_{k=1}^{\infty} \epsilon^k u_k(\mu, \eta), \qquad w = \sum_{k=1}^{\infty} \epsilon^k w_k(\mu, \eta), \qquad p = \sum_{k=1}^{\infty} \epsilon^k p_k(\mu, \eta). \tag{A.5}$$

To derive a fourth-order nonlinear model, we choose $\delta = 0$ $\gamma = 4$, and assume $\beta_2, \beta_3 = O(\epsilon^4)$ and $\nu = O(\epsilon^5)$, where $g \neq 0$ denotes the linear wave speed determined from the leading-order system.

Substituting (A.5) into (A.1)–(A.3) and collecting terms of equal powers of ϵ yields a sequence of systems at orders $O(\epsilon)$ through $O(\epsilon^5)$. We summarize below the key reduced systems needed to identify the nonlinear coefficients.

A.1. Leading-order systems:

At order $O(\epsilon)$, we obtain

$$\begin{aligned} &-2g\, u_{1\mu} + w_{1\mu} = 0, \\ &-g\, w_{1\mu} + p_{1\mu} = 0, \\ &p_1 = \beta_1 u_1. \end{aligned} \tag{A.6}$$

Setting

$$u_1(\mu, \eta) = U(\mu, \eta),$$

it follows that

$$w_1 = 2gU, \qquad p_1 = 2g^2 U, \tag{A.7}$$

and therefore

$$\beta_1 = 2g^2. \tag{A.8}$$

At order $O(\epsilon^2)$, the reduced system becomes

$$\begin{aligned} &-2g\,u_{2\mu} + w_{2\mu} + 3g(U^2)_\mu = 0,\\ &-g\,w_{2\mu} + 2g^2(U^2)_\mu + p_{2\mu} = 0,\\ &p_2 = \beta_1 u_2 + \beta_6 U^2. \end{aligned} \tag{A.9}$$

This yields

$$w_2 = 2gu_2 - 3gU^2, \qquad p_2 = 2g^2u_2 - 5g^2U^2, \tag{A.10}$$

from which we obtain

$$\beta_6 = -5g^2. \tag{A.11}$$

At order $O(\epsilon^3)$, the reduced system takes the form

$$\begin{aligned} &-2g\,u_{3\mu} + w_{3\mu} + 6g(Uu_2)_\mu - 4g(U^3)_\mu = 0,\\ &-g\,w_{3\mu} + 4g^2(Uu_2)_\mu - 6g^2(U^3)_\mu + p_{3\mu} = 0,\\ &p_3 = \beta_1 u_3 + 2\beta_6 Uu_2 + \beta_7 U^3. \end{aligned} \tag{A.12}$$

Hence,

$$w_3 = 2gu_3 - 6gUu_2 + 4gU^3, \tag{A.13}$$

and

$$p_3 = 2g^2u_3 - 10g^2Uu_2 + 10g^2U^3, \tag{A.14}$$

which gives

$$\beta_7 = 10g^2. \tag{A.15}$$

Similarly, at order $O(\epsilon^4)$, after simplification, one obtains

$$\begin{aligned} w_4 &= 2gu_4 - 6gUu_3 + 12gU^2u_2 - 5gU^4 - 3gu_2^2,\\ p_4 &= 2g^2u_4 - 10g^2Uu_3 + 30g^2U^2u_2 - \frac{35}{2}g^2U^4 - 5g^2u_2^2. \end{aligned} \tag{A.16}$$

Comparing this with the pressure expansion yields

$$\beta_8 = -\frac{35}{2}g^2. \tag{A.17}$$

A.2. Master equation:

At order $O(\epsilon^5)$, the solvability condition obtained from the reduced system leads to the master equation

$$4g^2U_\eta - 140g^2U^4U_\mu - \beta_4 gU_{\mu\mu} + (\beta_2 + g^2\beta_3)U_{\mu\mu\mu} - g\beta_5 U_{\mu\mu\mu\mu} = 0. \tag{A.18}$$

Dividing by $4g^2$ gives

$$U_\eta - a_1U^4U_\mu - a_2U_{\mu\mu} + a_3U_{\mu\mu\mu} - a_4U_{\mu\mu\mu\mu} = 0, \tag{A.19}$$

where

$$a_1 = 35, \qquad a_2 = \frac{\beta_4}{4g}, \qquad a_3 = \frac{\beta_2 + g^2\beta_3}{4g^2}, \qquad a_4 = \frac{\beta_5}{4g}.$$

Finally, after rescaling the stretched variables back to the original coordinates and dropping the scaling notation for simplicity, we obtain

$$u_t + a_1 u^4 u_x + a_2 u_{xx} - a_3 u_{xxx} + a_4 u_{xxxx} = 0. \tag{A.20}$$

Equation (A.20) represents a generalized nonlinear evolution equation with fourth-order nonlinearity. In particular, when $a_3 = 0$, it reduces to the GKS equation considered in this work:

$$u_t + a_1 u^4 u_x + a_2 u_{xx} + a_4 u_{xxxx} = 0. \tag{A.21}$$

Other well-known nonlinear evolution equations can also be recovered from (A.20) by suitable choices of the coefficients a_2, a_3, a_4.

AIMS Press